Hyperfine interactions in few-electron fluorine ions recoiling in gases

R. Brenn
Fakultät für Physik der Universität, 7800 Freiburg, Germany

F. Hopkins and G. D. Sprouse
Department of Physics, State University of New York, Stony Brook, New York 11794

(Received 21 October 1977)

The nuclear deorientation of $^{19}F(5/2_1^+$, 197 keV) has been measured for highly stripped fluorine ions recoiling in He, N_2, Ne, Ar, Kr, and Xe at 35 MeV and in N_2 and Ar at 55 MeV at gas pressures between 10^{-3} and 100 Torr. The nuclear alignment was found to decay quasiexponentially. The extracted nuclear deorientation cross sections are interpreted in a microscopic ion-atom collision model. The dominance of electronic charge-exchange transitions in producing the ionic states of strong hyperfine interactions is demonstrated. Collisional deexcitation of metastable states in heliumlike F is shown to contribute significantly.

I. INTRODUCTION

The strong hyperfine interactions in multiply ionized fast ions recoiling in gases have been exploited occasionally to measure magnetic moments of short-lived excited nuclear states.[1] For the heavy nuclei chosen in most of these experiments, the large number of charge and electronic states populated in the ion-atom collisions required the utilization of averages of atomic parameters such as hyperfine fields and collision times in order to interpret the measurements with a statistical model.[2] This statistical analysis is unsatisfying in that many questions are left unanswered concerning which classes of collisions or types of atomic states are important for the dealignment process. The model has no predictive power to aid in the choice of experimental parameters. For highly stripped light ions traveling in gases, however, the dominant electronic and charge states are few and it seems possible to analyze the nuclear deorientation in a more fundamental way by considering the specific atomic configurations and collision cross sections involved. The relative importance of charge-changing collisions versus inelastic excitation and collisional quenching for the deorientation can then be determined, and some insight into the important dealignment mechanism can be gained. This work shows that the dealignment can be qualitatively and quantitatively explained with a microscopic model based on collision cross sections, most of which have been measured in previous experiments.

In order to test the suitability of perturbed-angular-correlation (PAC) experiments of ion-atom collision studies we chose the collision systems F→ He, N_2, Ne, Ar, Kr, and Xe at ~2–3 MeV/amu where additional data from charge-exchange and x-ray work are available. As a nuclear probe the well-known $\frac{5}{2}{}_1^+$, 128-ns excited state of ^{19}F at 197 keV was chosen. In order to enable a comparison with the single-collision x-ray and charge-exchange measurements we measured the nuclear dealignment at low gas pressures under few-collision conditions.

In addition to the atomic physics aspects, systematic experiments of this kind are also important in providing a practical basis for selecting a gas environment in PAC measurements, where the nuclear alignment in fast ions is preserved or decays with a well-known time dependence.

In Sec. II a description of the experimental technique is given followed by the calculation of the perturbed γ-ray angular distribution in Sec. III. Section IV deals with the properties of the measured dealignment cross sections. In Sec. V the nuclear dealignment and its pressure dependence are interpreted in a microscopic collision model.

A preliminary account of this work has been given elsewhere.[3] The collision system 15-MeV ^{18}O in He has been studied in a similar PAC experiment in the high-gas-pressure region by Hagemeyer *et al.*[4]

II. EXPERIMENTAL TECHNIQUE

The $\frac{5}{2}{}_1^+$ state of ^{19}F at 197 keV ($\tau = 128$ ns, $g = 1.443$) was excited and strongly oriented by projectile Coulomb excitation of a ^{19}F beam. The anisotropy of the 197-keV decay radiation was measured as a function of gas pressure in a gas cell traversed by the ^{19}F ions. Figure 1 gives a schematic view of the experiment.

A ^{19}F beam of 50 or 65 MeV from the Stony Brook FN tandem accelerator is Rutherford scattered by a gold-target foil (thickness 1.8–3.4 mg/cm^2) into a cone centered at 40° to the beam direction. Part of the ^{19}F nuclei are projectile Coulomb

 © 1978 The American Physical Society

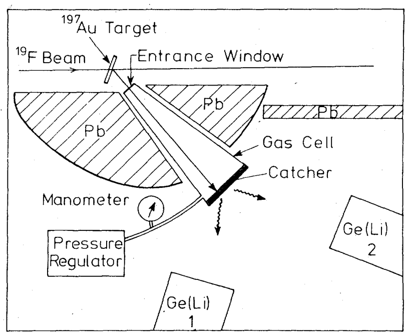

FIG. 1. Experimental setup.

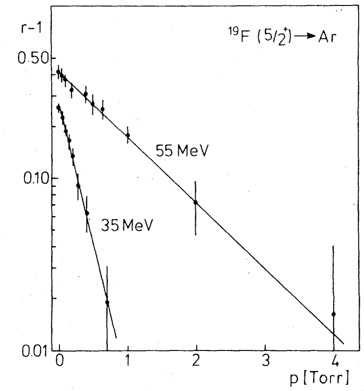

FIG. 2. γ-ray anisotropy $r-1$ [Eq. (2)] as function of gas pressure.

excited, strongly aligned, and polarized.[5] The scattered ^{19}F ions pass through a gas cell of 12 cm length where the hyperfine interactions in the free ions between gas collisions reduce the initial nuclear alignment, and are stopped in a copper sheet which essentially preserves the residual nuclear alignment until the γ decay.

The 197-keV decay radiation was measured by two large-volume Ge(Li) detectors positioned near the angles of maximum and minimum emission of the unperturbed angular distribution in the scattering plane (at 100° and 5° with respect to the beam direction; see Sec. III). The ratio r of both counting rates, which is a measure of the nuclear alignment remaining after passage through the gas cell, was recorded as a function of gas pressure.

Heavy lead shielding prevented projectile γ rays from ^{19}F ions scattered into all other solid angles from being registered in the detectors. Typical data-taking times were from 30 to 60 min for one gas pressure at beam currents of ~100-nA $^{19}F^{5+}$.

The conical gas cell of 12 cm length was separated from the accelerator vacuum by a 1.2-mg/cm^2 Ni entrance window. Gas pressures between 10^{-3} and 10^2 Torr were measured with a capacitance membrane manometer or a mechanical gauge, and kept constant to ~2% by a feedback-controlled needle valve. The energy transfer to the gold nuclei and the energy loss in gold target and Ni window foils resulted in mean ^{19}F energies of 35 and 55 MeV.

Figure 2 shows the anisotropy of the γ-rays deduced from the counting rate ratio r for 35 and 55 MeV ^{19}F in argon ($v/c = 0.061, 0.079$). An exponential decay of the alignment with increasing gas pressure is clearly visible. It will be discussed in Sec. III.

III. PERTURBED γ-RAY ANGULAR DISTRIBUTION

A. γ-ray angular distribution

The angular distribution of the emitted γ rays as a function of flight time t in the gas can be written

$$W(\theta_\gamma, \phi_\gamma, t) = 1 + \sum_{k=2,4} A_k Q_{kk} G_{kk}(\mathrm{Cu}) G_{kk}(t) \times \sum_{k=-k}^{+k} a_{kn} Y_{kn}(\theta_\gamma, \phi_\gamma) . \quad (1)$$

The lack of symmetry around the beam axis is responsible for the occurrence of the general spherical harmonics Y_{kn} instead of the usual Legendre polynomials.[6] Odd-k terms resulting from the nuclear polarization also produced in the Coulomb excitation process are omitted because the corresponding perturbation factors vanish for our case of isotropic perturbations and polarization-insensitive γ-ray detectors.[7] A_k are the angular correlation coefficients for the multipolarity $E2$ and spin sequence ($\frac{5}{2} \to \frac{1}{2}$) of our experiment ($A_2 = -0.535$, $A_4 = -0.617$). Q_{kk} and G_{kk}(Cu) are solid angle and copper attenuation coefficients, respectively [$G_{22}(\mathrm{Cu}) \approx 0.75$, $G_{44}(\mathrm{Cu}) \approx 0.75$ (Ref. 5)].

The statistical tensors a_{kn} were calculated with the Coulomb excitation code of Winther and de Boer.[8] θ_γ and ϕ_γ are the detector angles in the coordinate system of the a_{kn} coefficients. ($\theta_1 = \theta_2 = 90°$, $\phi_1 = 170°$, $\phi_2 = 75°$ in coordinate system 2 of Ref. 8; see also Fig. 1 of Ref. 9.) The attenuation coefficients $G_{kk}(t)$ will be discussed in Sec. III B.

The ratio of counting rates for both detectors, corrected for relative efficiencies $\epsilon_{1,2}$ can be written to a good approximation

$$r = \frac{\epsilon_2}{\epsilon_1} \frac{N(\theta_1, \phi_1)}{N(\theta_2, \phi_2)} = \frac{W(\theta_1, \phi_1)}{W(\theta_2, \phi_2)} \quad (2)$$

$$\approx 1 + a Q_{22} G_{22}(\mathrm{Cu}) G_{22}(t) \left(1 + b \frac{Q_{44} G_{44}(\mathrm{Cu}) G_{44}(t)}{Q_{22} G_{22}(\mathrm{Cu}) G_{22}(t)}\right) \quad (2')$$

$$= 1 + a' G_{22}(t) [1 + b' G_{44}(t)/G_{22}(t)] . \quad (2'')$$

From the statistical tensors a_{kn} of Eq. (1) for incident energies 50 and 65 MeV and 40° laboratory scattering angle one calculates $a \approx 0.5$ and $b \approx 0.25$. Therefore, $r-1$ measures essentially the perturbation factor $G_{22}(t)$ or, for a fixed flight time and varying gas pressure p, $G_{22}(p)$ (see Sec. III B). From Fig. 2 it can be noted that the measured $G_{22}(p)$ decreases exponentially with gas pressure p, i.e., with the number of gas collisions.

B. Perturbation factors $G_{kk}(t)$ and $G_{kk}(p)$

The perturbation of the nuclear alignment during recoil in vacuum or gas arises from the magnetic hyperfine interaction (hfi) $a_{IJ}IJ$ between the magnetic moment of the excited nuclear state and the ionic states, of angular momentum I and J, respectively. For the ion velocities of the present experiment the F ions exiting from the target or gas-cell-window foils are predominantly in charge states 9+ to 7+.[10] For the flight times between target, gas cell entrance and Cu stopper ($\langle t\rangle \approx 1-5$ ns) or between gas collisions (10 ps $\lesssim \langle t\rangle \lesssim$ 5 ns) in the pressure range of this experiment the nuclear dealignment is caused by either ionic ground states or metastable excited states of sufficiently strong hyperfine structure (hfs). For these states in the H-, He-, or Li-like F ions the interaction frequencies

$$\omega_{FF'} = [(a_{IJ} g_I)/(2\hbar)][F(F+1) - F'(F'+1)] \qquad (3)$$

are large enough to make $\omega_{FF'}\langle t\rangle \gtrsim 2\pi$, corresponding to a large nuclear precession between collisions. We neglect here any nuclear dealignment during electronic deexcitation cascades in the ions.

The attenuation factors between collisions thus reach their "hard-core" limit[6]

$$G_{kk}(J) = (2J+1)^{-1} \sum_F (2F+1)^2 \begin{Bmatrix} F & F & k \\ I & I & J \end{Bmatrix}^2 . \qquad (4)$$

Equation (4) is valid for isotropic hyperfine interactions. The hard-core attenuation factors are independent of t and the strength of the hfi and depend solely on I and the distribution $P(J)$ of ionic angular momenta J. Without gas collisions we have therefore

$$G_{kk}^{\text{vac}} = \sum_J P(J) G_{kk}(J) , \qquad (5)$$

the actual flight path being separated in two uncorrelated parts I and II (target–entrance-window, entrance-window–Cu stopper). The measured vacuum attenuation factor takes the form

$$G_{kk}^{\text{vac}}(\text{I}) G_{kk}^{\text{vac}}(\text{II}) , \qquad (5')$$

where $P_{\text{I}}(J)$ and $P_{\text{II}}(J)$ may be slightly different due to different ion velocities (energy loss in the entrance foil included) or foil materials. Comparison of measured vacuum attenuation factors with calculated ones using measured charge state distributions $P(\phi)$ should allow the determination of average metastable fractions (e.g., $^3S_1$ in F^{7+}) produced in foil excitation. The lack of time information and the insensitivity of G_{kk}^{vac} to $\omega_{FF'}$ make this technique, however, less sensitive than time-resolved plunger experiments.[11]

The calculation of the attenuation factor $G_{kk}(t,p)$ for gas collisions (flight-path part II) can be performed with the existing theories of statistically perturbed angular correlations.[6,12,13] Whereas the limiting case of high pressure ($\omega_{FF'}\tau_c \ll 1$, τ_c being the correlation time of gas collisions) leads to the well-known exponential relaxation of the nuclear alignment and γ-ray anisotropy (Abragam-Pound relaxation[6]), the calculations of $G_{kk}(t,p)$ for $\omega_{FF'}\tau_c \lesssim 1$ but not $\ll 1$ are tedious and only possible numerically,[4,12,13] except for the limiting case of large t.[13]

Guided by the experimentally observed quasi-exponential decay of alignment (Fig. 2) in the few-collision low-pressure regime of the present experiment, one expects such a behavior to follow in the hard-core limit of statistical perturbations, i.e., for $\omega_{FF'}\tau_c \gtrsim 2\pi$ between collisions, where the attenuation factor of Eq. (4) is inserted between collisions.

Using techniques of ordering according to the number of collisions and Laplace transformation[13] it is possible[14] to derive the following approximate expression for $G_{kk}(t)$ in the case of hard-core gas collisions:

$$G_{kk}(t) = G_{kk}^{\text{vac}} e^{-r_k t} \qquad (6)$$

with G_{kk}^{vac} taken from Eq. (5) and r_k given by

$$r_k = (1/\tau_c)[1 + \tfrac{1}{2}a_k - \tfrac{1}{2}(a_k^2 - 4b_k)^{1/2}] \qquad (7)$$

with

$$\tau_c = 1/n(p)v\sigma ,$$

$$\sigma = \sum_{i,j} P(J_i)\sigma(i \to j) ,$$

$$a_k = -\sum_i G_{kk}(J_i) W_{ii} ,$$

$$b_k = \sum_{i<j} G_{kk}(J_j)(W_{ii}W_{jj} - W_{ij}W_{ij}) G_{kk}(J_i) .$$

The above derivation of $G_{kk}(t)$ holds for a system of levels $|i\rangle$, $|j\rangle$ with angular momenta J_i, J_j, and collision-induced transitions $i \to j$ with cross sections $\sigma(i \to j)$ and branching ratios

$$W_{ij} = \sigma(i \to j) \Big/ \sum_j \sigma(i \to j) .$$

v is the ion velocity and $n(p)$ the gas density.

Whereas $\sigma(i\to j)$, $i\neq j$ describes a transition between different ionic states $|J_i\rangle$, $|J_j\rangle$, $\sigma(i\to i)$ is used to include "spin-flip" transitions with $\Delta m_{J_i}\neq 0$ within the same state $|J_i\rangle$.

Explicitly one has the following pressure dependence of G_{kk} for a fixed flight time $t=d/v$, d being the gas cell length:

$$G_{kk}(p)=G_{kk}^{\mathrm{vac}}\exp\{-n(p)d\sigma[1+\tfrac{1}{2}a_k-\tfrac{1}{2}(a_k^2-4b_k)^{1/2}]\} \quad (8)$$

$$=G_{kk}^{\mathrm{vac}}e^{-p/p_k} \quad (8')$$

$$=G_{kk}^{\mathrm{vac}}e^{-N/N_k} \quad (8'')$$

P_k and N_k (atoms/cm^2) are the pressure and target thickness, respectively, for alignment $G_{kk}^{\mathrm{vac}}e^{-1}$.

As in the Abragam-Pound case of small nuclear precession between collisions, the opposite limit of large precession leads to an exponential decay (quasirelaxation) of the alignment with time. The decay constant r_k is, however, independent of the strength of the hfi. The two experimentally observable quantities, G_{kk}^{vac} and r_k (or p_k, N_k), contain averages over ionic state distributions $P(J_i)$ and individual cross sections $\sigma(i\to j)$ for ionization, charge exchange, excitation, and quenching or spin-flip processes. Even for a small number of participating levels it is not possible to deduce individual $\sigma(i\to j)$ from the data even when additional information on most of the cross sections (like charge exchange or ionization involving ionic ground states) is available. It is, however, possible to deduce average quantities of interest like magnitude of quenching or excitation cross sections involving metastable levels as will be demonstrated in Sec. V.

IV. Z AND v DEPENDENCE OF NUCLEAR DEALIGNMENT

The measured gas-pressure dependence of the counting rate ratio r is shown in Figs. 3 and 4 for the collision systems 35 and 55 MeV in He, N_2, Ne, Ar, Kr, and Xe. The full curves are least-squares fits using the function of Eq. (2′) and the attenuation factor $G_{22}(p)$ from Eq. (8). The small correction term containing $G_{44}(p)$ was included approximately by using a numerical relation between G_{44} and G_{22}, roughly valid for magnetic hyperfine interactions [$G_{44}\approx \alpha G_{22}+(1-\alpha)(G_{22})\kappa$ with $\alpha\approx 0.5$, $\kappa\approx 4$–8]. The influence of α and κ on the results of the fits was smaller than the statistical errors.

The results obtained for the initial anisotropy a' and for the characteristic decay cross section $S=1/N_2$ are given in Table I. From Eq. (8) it follows that

$$S=\sigma(1+\tfrac{1}{2}a_2-\tfrac{1}{2}(a_2^2-4b_2)^{1/2}. \quad (9)$$

S is therefore the average collision cross section

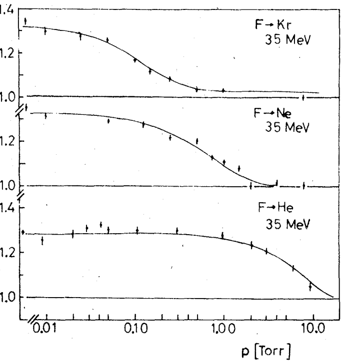

FIG. 3. Counting rate ratio r as function of gas pressure for F→ He, Ne, Kr, with fits obtained with the function of Eq. (2″).

weighted with a factor that describes the average influence of a collision of the γ-ray anisotropy, governed by hard-core attenuation factors $G_{kk}(J)$ and branching ratios to states $|J\rangle$.

The dependence of S on the target Z is shown in Fig. 5 for 35 MeV incident F energy. There is a strong monotonic increase with Z except for the anomalously low Xe value. A comparison with measured electron-capture cross sections for F → Ar, Kr, Xe at 35.7 MeV,[15] which show the same increase and anomaly, suggests the importance of charge-exchange processes in populating the ionic states relevant in the present experiment.

The decrease of S with ion velocity (see Table I, 35 and 55 MeV values) is consistent with the strongly decreasing capture cross sections for F in N_2 (Ref. 16) and Ar (Ref. 17) although an additional weak velocity dependence arises from the change in the angular momentum or charge state distribution with velocity.

V. MICROSCOPIC MODEL OF NUCLEAR DEORIENTATION

The charge state distributions $P(\phi)=(\phi_9,\phi_8,\phi_7,\phi_6)$ of F ions entering the gas cell after passing through the entrance window can be estimated[10] to

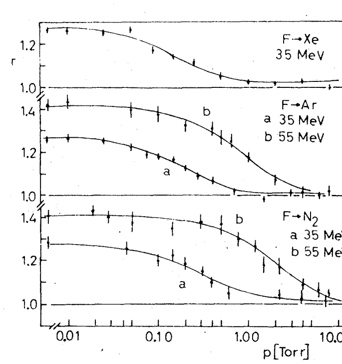

FIG. 4. Same as Fig. 3, for F→ N_2, Ar, Xe.

TABLE I. Zero-pressure anisotropy a' [Eq. (2″)], characteristic pressure p_2 [Eq. (8′)], target thickness N_2 [Eq. (8″)], and deorientation parameter $1/N_2$ obtained from fits and model calculations.

Case	E_i (MeV)	a'	p_2 (Torr)	$N_2(10^{18}\ \mathrm{cm}^{-2})$	Measured $1/N_2(10^{-18}\ \mathrm{cm}^2)$	Calculated Case a[b]	Case b[c]	Case c[d]
He	35	0.29[a]	7.6(10)	3.5(4)	0.29(4)	...[e]	...[e]	...[e]
N_2	35	0.25(3)	0.36(7)	0.16(3)	6.2(13)	0.94	1.7	3.6
N_2	55	0.39(2)	2.65(36)	1.21(16)	0.83(11)	0.43	0.77	1.3
Ne	35	0.33(2)	0.81(13)	0.37(6)	2.7(4)	...[e]	...[e]	...[e]
Ar	35	0.27(1)	0.260(25)	0.12(1)	8.5(8)	2.4	3.8	6.3
Ar	55	0.40(3)	1.08(16)	0.49(7)	2.0(3)	1.3	2.2	3.3
Kr	35	0.29(2)	0.156(12)	0.07(6)	14.1(11)	4.8	6.3	11.7
Xe	35	0.26(2)	0.211(35)	0.10(2)	10.4(17)	3.4	5.7	10.5

[a] Kept fixed.
[b] $P(7^*)=0,\ \sigma_{i7}=0$.
[c] $P(7^*)=P(7),\ \epsilon=0.5,\ \sigma_{7^*7}=0$.
[d] $P(7^*)=P(7),\ \epsilon=0.5,\ \sigma_{7^*7}=2\sigma_{7^*8}$.
[e] Charge exchange cross sections not available.

be (0.56, 0.35, 0.09, 0.00) at 55 MeV and (0.12, 0.48, 0.36, 0.04) at 35 MeV. Although $\langle\phi\rangle$ will be lowered by the capture processes in gas we consider only bare H-, He-, and Li-like ions. In addition to the ionic ground states we include the metastable $^3S_1$ state of F^{7+} in the $P(J_i)$ distribution because metastable states are strongly populated in beam-foil excitation.[11] Other excited ionic states are not considered here because either they are too weakly populated (e.g., the potentially important ^4P_J state of the F^{6+} is at most populated a few percent of the 0.04 charge fraction, and was neglected), or too short lived to cause appreciable nuclear deorientation ($^3P_1$, etc.), or because they have the same J_i and $G_{kk}(J_i)$ as the ground state ($2\,^2S_{1/2}$ of F^{8+}, $^1S_0$ of F^{7+}) or their hfi is too weak to perturb the nuclear alignment in the time scale considered here. In view of the small number (two) of experimentally determined parameters it is necessary to keep the number of model levels at a minimum.

The calculation of $G_{kk}(p)$ from Eq. (8) was performed in the five-level model with the level specifications given below:

$|6\rangle$: F^{6+}, $2\,^2S_{1/2}$; $J=\frac{1}{2}$, $G_{22}=0.833$, $G_{44}=0.444$;

$|7\rangle$: F^{7+}, $(1s)^2\,^1S_0$, $(1s2s)\,^1S_0$; $J=0$, $G_{22}=G_{44}=1$;

$|7^*\rangle$: F^{7+}, $(1s2s)\,^3S_1$; $J=1$, $G_{22}=0.609$, $G_{44}=0.156$;

$|8\rangle$: F^{8+}, $^2S_{1/2}$; $J=\frac{1}{2}$, $G_{22}=0.833$, $G_{44}=0.444$;

$|9\rangle$: F^{9+}; $J=0$, $G_{22}=G_{44}=1$.

The factors G_{kk} are the hard-core attenuation factors for $I=\frac{5}{2}$ and J specified above, calculated from Eq. (4). For these levels and the pressure range of our experiment the hard-core condition $\omega_{FF'}\tau_c \gtrsim 2\pi$ is always fulfilled.

The counting rate ratio r at zero pressure [Eqs. (1) and (2) with G_{kk} taken from Eqs. (5′) and (5)] contains the J distribution $P(J_i)$, $i=6,\ 7,\ 7^*,\ 8,\ 9$. Owing to the uncertainties in the perturbation factors $G_{kk}(\mathrm{Cu})$ and charge state distributions, the metastable fractions $P(7^*)/[P(7)+P(7^*)]$ cannot be extracted very accurately. Fractions of 0.5 ± 0.3 (Refs. 9 and 11) are consistent with the fitted amplitudes a' (Table I) for 35 and 55 MeV incident energy. The 55-MeV initial anisotropies are larger than the 35-MeV values because of the larger fraction $P(9)$ of F^{9+} with zero hfi; the weak energy dependence of the Coulomb excitation tensors a_{kn} in Eq. (1) contributes little.

The corresponding collision cross sections $\sigma(i\rightarrow j)$ can be divided into the groups (a) single- or multiple-electron capture: σ_{98}, σ_{87^*}, σ_{87}, σ_{7^*6}, σ_{76}; σ_{97}, etc.; (b) ionization: σ_{67}, σ_{78}, σ_{7^*8}, σ_{89}; σ_{68}, etc., (c) excitation or deexcitation (quenching): σ_{77^*}, σ_{7^*7}, etc., (d) "spin-flip" processes

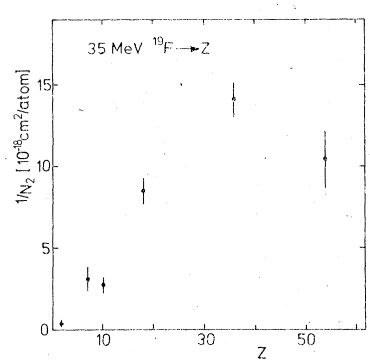

FIG. 5. Z dependence of deorientation parameter $1/N_2$.

or reorientation: σ_{66}, etc., with $\Delta m_J \neq 0$, (e) higher processes: ionization or capture accompanied by excitation, etc.

Single- and multiple-charge exchange or ionization cross sections are known for most of the collision systems studied here.[15-17] Whereas these published capture cross sections include capture into excited states (e.g., σ_{87*}), the corresponding loss cross sections are assumed to represent electron loss from the ground states only.

For the five-level system, 12 of the possible 25 collision cross sections $(i \to j)$ are known from charge-exchange work[15-17]: $\sigma_{67}+\sigma_{67*}$, σ_{68}, σ_{69}, σ_{76}, σ_{78}, σ_{79}, σ_{86}, $\sigma_{87}+\sigma_{87*}$, σ_{89}, σ_{96}, $\sigma_{97}+\sigma_{97*}$, σ_{98}. The small strength of spin-dependent interactions compared to Coulomb interaction for the fast collisions encountered in the present experiment suggests neglecting the spin reorientation cross sections σ_{88}, σ_{7*7*}, σ_{66} (with $\sigma_{99}=\sigma_{77}=0$) against ionization or capture cross sections. The same argument leads to a negligibly small expected singlet-triplet excitation cross section $\sigma_{77*}=\beta\sigma_{78}$ with $\beta \ll 1$.

As model parameters we chose the ratio $\epsilon=\sigma_{87*}/(\sigma_{87}+\sigma_{87*}) \approx \sigma_{97*}/(\sigma_{97}+\sigma_{97*})$ of electron capture into $F^{7+}(^3S_1)$ to ground-state capture and the ratio $\alpha = \sigma_{7*7}/\sigma_{7*8}$ of $^3S_1$ quenching to ionization. Finally we set $\sigma_{67*} \approx \frac{1}{2}\sigma_{78}$, $\sigma_{7*6} \approx \frac{1}{2}\sigma_{87}$, $\sigma_{7*8} \approx \sigma_{67}$, $\sigma_{7*9} \approx \sigma_{68}$ because of the similarity of the processes involved, the factors $\frac{1}{2}$ arising from statistical arguments. These approximations are justified by the large (~30%) quoted errors of the charge-exchange cross sections of Refs. 15–17.

The decay constant of the γ-ray anisotropy $1/N_2$ obtained from the experiment (see Table I) can now be reproduced by the set of collision cross sections given above, with the capture ratio ϵ into the heliumlike $^3S_1$ state and the quenching ratio $\beta = \sigma_{7*7}/\sigma_{7*8}$ chosen as parameters. For $\sigma(i \to i)=0$ (no spin-flip processes) one obtains from Eq. (7)–(8′)

$$\frac{1}{N_2} = \sigma\left[1-\left(\sum_{i<j} G_{22}(J_i)G_{22}(J_j)W_{ij}W_{ji}\right)^{1/2}\right] = \sigma f_2 \tag{10}$$

with $\sigma = \sum_{i,j} P(J_i)\sigma(i \to j)$. $1/N_2$ was calculated for three sets of parameters: (a) $^3S_1$ state not included: $P(7^*)=0$, and cross sections populating this level are assumed zero. (b) $^3S_1$ state included with $P(7^*)=P(7)$, $\epsilon=\sigma_{87*}/(\sigma_{87}+\sigma_{87*})=\frac{1}{2}$, but $\sigma_{7*7}=0$ (no quenching included). (c) Same as (b), but quenching included with $\sigma_{7*7}=2\sigma_{7*8}$. In all cases spin-flip processes $(\sigma_{ii}, \sigma_{77*})$ are neglected.

The results of the calculations are given in Table I. It can be noted that the calculated deorientation cross sections $1/N_2$ for case (a) (no metastable states included) are significantly smaller than the measured values, even when the uncertainties of the charge state distribution and charge-exchange cross sections are taken into consideration. Case (b) ($^3S_1$ state included; no quenching) seems to reproduce the higher-energy data (55 MeV) whereas it still results in too small a deorientation for the 35-MeV data. Variation of the $^3S_1$ foil excited fraction and of the $^3S_1$ to $^1S_0$ capture ratio ϵ can account for a part of this additional deorientation only. The most likely process increasing the collision cross section is $^3S_1$ to $^1S_0$ deexcitation (quenching). The magnitude of σ_{7*7} required to reproduce the 35-MeV data $[\sigma_{7*7} \approx (3-4)\sigma_{7*8}$ or $(3-4)\sigma_{67}]$ does not seem unreasonable (cf. Refs. 1 and 19 for large metastable quenching cross sections in fast He→gas collisions). In view of the various assumptions underlying the present collision model (e.g., relations between some of the unknown σ_{ij} involving charge exchange from or to the $^3S_1$ level) it is not reasonable to quote a more precise number for σ_{7*7} as could be obtained from a fit to the data.

It has been demonstrated that the phenomenon of nuclear deorientation in fast, few-electron ions traveling in low-pressure gas can be understood qualitatively and quantitatively in a model which uses collision-induced cross sections between a small number of ionic states as parameters. When supplied by additional data from direct measurements (e.g., charge-exchange, x-ray, or Auger data) the present technique may complement these techniques in gaining information on fast ion-atom collision phenomena, specifically processes involving population and destruction of metastable states.

ACKNOWLEDGMENTS

The authors would like to thank Dr. L. E. Young, Dr. A. R. Whittemore, Dr. G. Yue, Dr. J. Lin, and Dr. Joel Karp for their help during some of the experiments, and H. Kolb for the use of his calculations. This research was supported in part by the National Science Foundation.

[1]See, e.g., M. B. Goldberg, Phys. Scr. 11, 184 (1975), and references therein.
[2]See, e.g., R. Brenn, H. Spehl, A. Weckherlin, H. A. Doubt, and G. van Middelkoop, Z. Phys. A 281, 219 (1977), and references therein.
[3]R. Brenn, F. Hopkins, and G. D. Sprouse, Hyperfine Interactions 2, 393 (1976).
[4]K. Hagemeyer, M. B. Goldberg, G. J. Kumbartzki,

K.-H. Speidel, P. N. Tandon, M. Schramm, and G. Kraft, Hyperfine Interactions 1, 301 (1975).

[5]G. D. Sprouse, R. Brenn, H. A. Calvin, and H. J. Metcalf, Phys. Rev. Lett. 30, 419 (1973).

[6]R. Steffen and H. Frauenfelder, in *Perturbed Angular Correlations,* edited by E. Karlsson, E. Matthias, and K. Siegbahn (North-Holland, Amsterdam, 1964).

[7]L. Grodzins and O. Klepper, Phys. Rev. C 3, 1019 (1971).

[8]A. Winther and J. de Boer, in *Coulomb Excitation,* edited by K. Alder and A. Winther (Academic, New York, 1966).

[9]R. Brenn, G. D. Sprouse, G. Yue, and O. Klepper, Nucl. Phys. A 265, 35 (1976).

[10]J. Marion and F. Young, *Nuclear Reaction Analysis* (North-Holland, Amsterdam, 1968), p. 44.

[11]See, e.g., R. E. Horstman, J. L. Eberhardt, H. A. Doubt, C. M. E. Otten, and G. van Middelkoop, Nucl. Phys. A 248, 291 (1975).

[12]C. Scherer, Nucl. Phys. A 157, 81 (1970); M. Blume, Nucl. Phys. A 167, 81 (1971).

[13]F. Bosch and H. Spehl, Z. Phys. 268, 145 (1974); Hyperfine Interactions 1, 255 (1975).

[14]H. Kolb, diploma thesis (Universität Freiburg, 1976) (unpublished); R. Brenn and H. Kolb (unpublished).

[15]J. R. Macdonald, L. Winters, M. D. Brown, T. Chiao, and L. D. Ellsworth, Phys. Rev. Lett. 29, 1291 (1972).

[16]J. R. Macdonald, S. M. Ferguson, T. Chiao, L. D. Ellsworth, and S. A. Savoy, Phys. Rev. A 5, 1188 (1972).

[17]S. M. Ferguson, J. R. Macdonald, T. Chiao, L. D. Ellsworth, and S. A. Savoy, Phys. Rev. A 8, 2417 (1973).

[18]E. H. Pedersen, Phys. Rev. A 15, 53 (1977).

[19]R. J. Fortner and D. L. Matthews, Phys. Rev. A 16, 1441 (1977).